James Madison University
JMU Scholarly Commons

Senior Honors Projects, 2010-current   Honors College

Spring 2019

Multi-proxy characterization of ACEX subunit 1/5 (the "zebra" interval) to better understand sediment deposition at this critical age boundary and paleoceanographic transition

Victoria Hojnacki

Follow this and additional works at: https://commons.lib.jmu.edu/honors201019

Part of the Geology Commons

Multi-proxy Characterization of ACEX Subunit 1/5 (the "Zebra" interval) to Better Understand

Sediment Deposition at this Critical Age Boundary and Paleoceanographic Transition

_____

An Honors College Project Presented to

the Faculty of the Undergraduate

College of Science and Mathematics

James Madison University

_____

by Victoria Marie Hojnacki

April 2019

Accepted by the faculty of the Department of Geology & Environmental Science, James Madison University, in partial fulfillment of the requirements for the Honors College.

FACULTY COMMITTEE: HONORS COLLEGE APPROVAL:

_____   _____
Project Advisor: Kristen E. St. John, Ph.D.   Bradley R. Newcomer, Ph.D.,
Professor, Department of Geology & Environmental   Dean, Honors College
Science

_____
Reader: Stephen A. Leslie, Ph.D.
Department Head, Department of Geology &
Environmental Science

_____
Reader: John T. Haynes, Ph.D.
Associate Professor, Department of Geology &
Environmental Science

PUBLIC PRESENTATION

This work is accepted for presentation, in part or in full, at the James Madison University Honors Symposium on 5 April 2019.

In dedication to my parents, Patrick Jerome Hojnacki and Susan Marie Kent, who have made it possible for me to receive a wonderful education and have encouraged me to follow my interests wherever they lead me.

Table of Contents

List of Figures

Figures

Acknowledgements

I would like to acknowledge and thank Dr. Kristen St. John for being my research advisor and introducing me to the subject area of paleoceanography and paleoclimatology. The support you provided was integral in the completion of this project and in my decision to pursue a graduate degree. I would also like to thank Dr. Stephen Leslie and Dr. John Haynes for being readers on my Honors capstone project. I am grateful for the feedback you have provided on my research. I greatly appreciate the assistance that Zach Strasberg provided in preparing samples for analysis. Thank you for taking the time to help me with my project. Lastly, I would like to thank Jeffery E. Tickle for his investment in the College of Science and Mathematics, which provided me with funding from the Jeffrey E. Tickle '90 Family Endowment in Science & Mathematics. This funding allowed me to begin my senior research the summer before my senior year. This additional time to complete work made it possible to submit an abstract for the 2018 American Geophysical Union Fall Meeting.

Abstract

Sediment cores recovered from the Lomonosov Ridge on IODP Expedition 302, the Arctic Coring Expedition (ACEX), provided the first major insights into long-term Cenozoic history of climate and ocean conditions in the central Arctic. However, the ACEX record is hampered by a major hiatus or severely condensed interval (depending on age-model interpretations) at 198.7 mcd separating the middle Eocene and Miocene records. Lithologic subunit 1/5 lies above this depth horizon, and is informally called the "zebra interval" because of distinctive stripes - black and gray tilted and cross-banded silty-clay layers, up to 3 cm thick that characterize the lower ~2.5 m of the subunit. Prior studies provide micropaleontological evidence for a brackish, shallow water depositional environment below and across the hiatus, continuing into subunit 1/5; and the cross-banding suggests a high-energy shallow water setting conducive to reworking and erosion. In addition, prior studies place the hiatus and subunit 1/5 within an overall up-section transition from warmer to cooler temperatures with more persistent ice-rafting, and from restricted to more open water circulation. Given the paleoclimatic and paleoceanographic differences above and below this interval and its unique lithologic pattern, this study aimed to better characterize the sedimentology of the black and gray couplets.

Twenty-four samples from the black and gray layers and eleven samples from above and below the "zebra interval" were analyzed to characterize the XRF elemental composition, XRD bulk and clay mineral composition, grain size, and coarse sand composition and abundance. Overall, the zebra interval had less Fe and more variability in grain size than the stratigraphic intervals above and below it. In addition, the zebra interval showed upcore shifts from smectite to illite-dominated clays and greater abundance of terrigenous coarse sand. The sand-sized grains are quartz-dominated, showing very little change in composition throughout all three of the

lithologic sub-units. Quartz-grains are also generally well-rounded. Differences between the gray and black layers within the zebra interval were limited; gray bands tended to have greater abundances of quartz and muscovite, slightly higher Ti abundances, and lower abundances of Fe, Co, Ni, K, P, As, Sr, and Mn than the black layers.

The sedimentological observations are perplexing. Rounded quartz suggests reworking in a shallow water setting that has wave or tide action, so this, along with the tilted and cross-banding support the micropaleontological interpretation of an estuarine depositional setting for the zebra interval. The compositional differences (abundance of quartz and muscovite) may indicate semi-regular differences in transport energy or provenance that could relate to variations in input due to seasonal changes, storms or tides. However, the duration of a black-gray couplet is unknown, making it difficult to infer a specific depositional control. Complicating this further is the lack of graded bedding or other distinct changes in grain size between the gray and black layers, which would be expected if shallow water currents produced the tilted and cross-bedded layers. However, these inconsistencies may be artifacts of the sample processing – the samples were semi-lithified and therefore difficult to disaggregate. Additional grain size work that does not require disaggregation should be conducted. The dominance of the clay mineral smectite in subunit 1/5 suggests transport from the Kara and/or Laptev Sea regions.

An alternative interpretation for the origin of the black and gray layers is that the color changes could be the result of post-depositional semi-regular changes in oxidation of the bottom waters. In an estuary this might occur due to seasonal overturn, and could be sea-ice influenced However, this is difficult to reconcile with the tilted and cross-bedded nature of the black and gray layers.

At a broader scale, the distinct shift in clay mineralogy and drop in sand abundance from subunit 1/5 ("zebra interval") to overlying subunit 1/4 may indicate a change in circulation from a strong transpolar drift current to an increase in terrigenous transport to the central Arctic by the Beaufort Gyre. This puzzling time of paleoceanographic and paleoclimatic transition will be investigated further in upcoming IODP Expedition 377.

1. Introduction

1.1 Background

In September of 2004, the Integrated Ocean Drilling Program (IODP) Expedition 302 (commonly called ACEX) set out to obtain a continuous sedimentary record showing the paleoenvironmental evolution of the Central Arctic Ocean. The drilling location, ~88°N, 140°E, is about 250 km from the North Pole, along the Lomonosov Ridge (figure 1). Prior to the expedition, the Lomonosov Ridge was mapped using seismic reflection and refraction data, which showed that the ridge was likely comprised of undisturbed, flat-lying strata. This expedition gave the first insight into the long-term Cenozoic history of the Arctic Ocean.
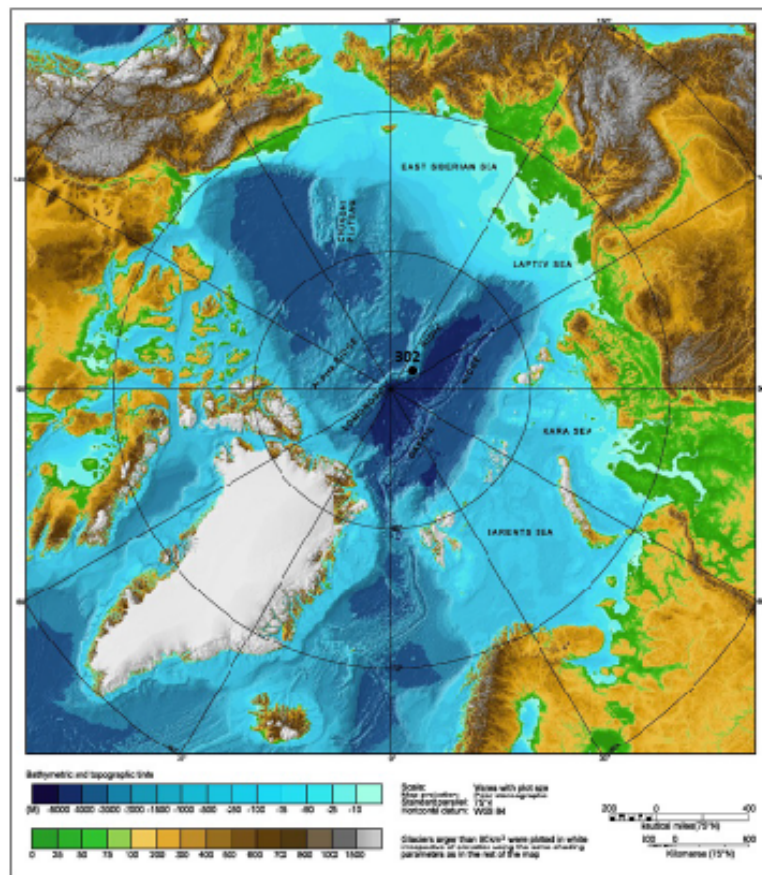

Figure 1: Arctic Ocean with IODP Expedition 302 site locations noted (Modified from NOAA; http://www.ngdc.noaa.gov/mgg/bathymetry/arctic/provisionalmap.html).

At a water depth of ~ 1,300 meters, the expedition recovered sediment cores reaching depths of 428 meters below the seafloor (mbsf). Cores were taken from four different sites and were correlated using several datasets, including seismic data, biostratigraphy, and lithostratigraphy. The record recovered extends back to the Late Cretaceous; however, within the record two depositional hiatuses are present. The longer and older of the two hiatuses occurs at 193.13 mbsf and spans 25 million years, according to the expedition report (Expedition 302 Scientists, 2006). The hiatus occurs at a division between two modes of sedimentation. The sediments below the hiatus are rich in organics and siliceous microfossils, which is indicative of deposition in a euxinic and anoxic setting, while the fossil-poor silty clays deposited following the hiatus suggest an ice-dominated setting (O'Regan et al., 2008). The sediments immediately above and below this hiatus are the focus of my undergraduate research. These sediments include a section called the "zebra interval", named for its black and dark gray layering, which give the appearance of stripes.

1.2 Sample Stratigraphy

Samples were obtained from the IODP Bremen Core Repository for use in this study. The sampling strategy aimed to get representative samples from above, within, and below the "zebra interval", including samples from the black and gray zebra stripes (Figure 2). In total, 35 samples of ~10 cc volume were available for analyses (Appendix A) from the three different subunits shown in figure 2. As reported in the expedition findings (Expedition 302 Scientist, 2006), the fundamental characteristics of samples in Subunits 1/4 through 1/6 are summarized below.

Subunit 1/4

Samples taken from Expedition 302 Site 2 Hole A Core 46 are above the "zebra interval" and are middle Miocene in age. The lithology is silty clay, which alternates in color from dark

brown to grayish brown. The sediment is poor in organic carbon and microfossil content. The subunit is rich in dropstones and sand lenses.

Subunit 1/5

Samples taken from Expedition 302 Site 2 Hole A Core 45 are part of the "zebra interval" and are middle to early Miocene in age. The interval is characterized by black to dark gray, alternating clayey bands. Packages of stripes are tilted. The light portions of the interval are more oxidized while the darker portions are less oxidized (Sangiorgi et al., 2008). Since the initial recovery of the core, the colors of the "zebra interval" have faded, as noted by scientists at the Bremen Core Repository. This was taken into consideration when selecting the samples. Some shifts in the sampling were made to avoid oversampling this critical interval, and to ensure that samples were taken in the color distinct bands.

Subunit 1/6

Samples taken from Expedition 302 Site 2 Hole A Core 44 are below the "zebra interval" and are middle Miocene to middle Eocene in age. The sediments are dark, siliciclastic silt that is rich in organic carbon, and they contain pyrite and microfossils. Isolated pebbles are also seen in this subunit. Three of the five samples received from this core were shifted from the intervals requested. These shifts were to avoid oversampling of an area of the core.

Post-Recovery Gypsum

When sampling of the core was completed in January 2018, scientists from the IODP Bremen Core Repository documented gypsum crystals on the surface of the core. Gypsum ($CaSO_4 \cdot 2H_2O$) is not typically found in deep marine sediments because the ocean is undersaturated in gypsum (St. John et al., 2000). Therefore, the gypsum present on (and

13

potentially in) the core probably formed as a precipitate after core recovery, while in the storage

at the core repository. Likely, the seawater present in the core sediments following recovery

evaporated, and the calcium sulfate salts precipitated as gypsum. However, in 2009, Kaminski

noted some interspersed gypsum in the core, which was attributed to subaerial exposure on the

Lomonosov Ridge. This could mean that gypsum is not only present on the surface, and that

some of it could be primary.

Figure 2: Left- Lithologic stratigraphic column (Expedition 302 Scientists, 2006). Right – Photographs of the cores being examined in this study. The red dots represent the samples received and the blue dots are data points from St. John (2008).

2. Paleoenvironmental Setting of the Lomonosov Ridge

2.1 Subsidence History

There is scientific controversy and uncertainty regarding the hiatus and the subsidence history of the Lomonosov Ridge. In order to explain the 25-million-year hiatus identified in the core recovered during the expedition, subsidence models of the Lomonosov Ridge were developed (Moore et al., 2006). Currently the Lomonosov Ridge is located in the central Arctic, but ~57 million years ago it was a part of the Eurasian continental margin, and for approximately 2 million years following rifting, the ridge remained in neritic conditions before subsidence began (Moore et al., 2006). This subsidence was caused by post-rift cooling. Throughout its history, the ridge's depth below sea level also varied with changes in global sea level. Over the past 54 million years, the ridge has drifted away from the Eurasian margin, and subsided to its current depth.

The subsidence hypothesis of Moore et al. (2006) attributes the hiatus at 193.13 mbsf to an increase in strong bottom currents (at >1000 m paleodepth) that eroded, reworked, and then redeposited the upper Eocene and Oligocene sediments, a process that is interpreted as having produced sand lenses and cross-bedding observed by the shipboard scientific party (Expedition 302 Scientists, 2006). In contrast, other scientists (Sangiorgi et al., 2008; Kaminski 2009) have hypothesized that the subsidence history was different, and that it included a lengthy period when the ridge was in shallow water, either at or near sea level. Such an environmental setting would promote wave erosion and/or non-deposition, thereby producing the hiatus. Supporting this shallow model are palynological, micropaleontological, and geochemical data (Figure 3; Sangiorgi et al., 2008). In particular, the presence of fungal and fern spores both below and above the hiatus is consistent with an environment at or near sea level (Sangiorgi et al., 2008). A

third variation on the paleoenvironmental history of the Lomonosov Ridge is one that allows for

its early subsidence, but with that episode of subsidence then followed by uplift to above sea

level, all of which is the result of regional tectonic movements associated with the rifting of the

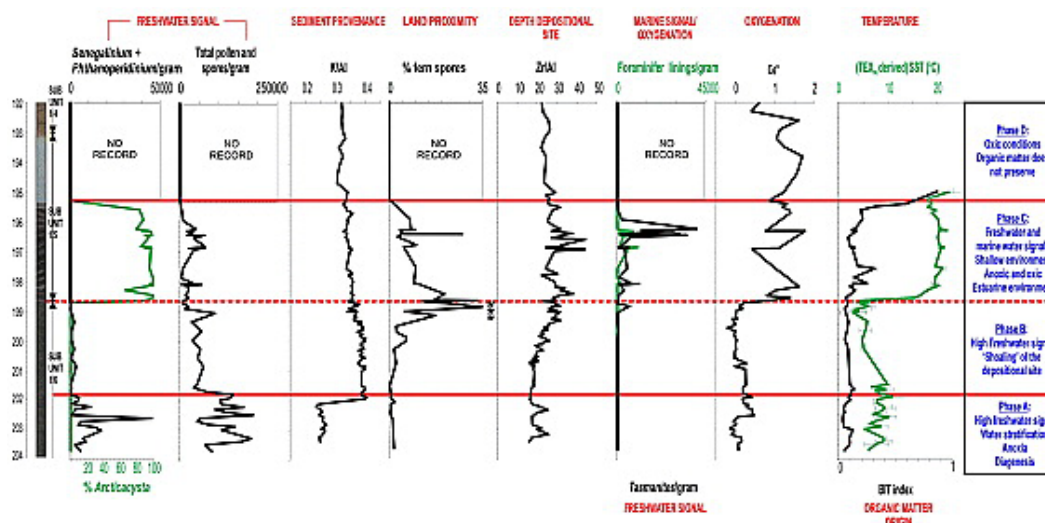Yermak and Morris Jesup Plateaus at ~33 Ma (Kaminski 2009).

Figure 3: Summary diagram from Sangiorgi et al (2008) showing changes in a range of paleoenvironmental proxy data across the primary hiatus (indicated by the dashed line) in the ACEX sediment record.

2.2 Age-Depth-Model

In addition to the subsidence history, there is also controversy surrounding the age-depth

model of the Lomonosov Ridge. The two current models differ in methods and in their

interpretation of the hiatus. Backman et al. (2008) developed an age-depth model based on

micropaleontology, beryllium isotope stratigraphy, and paleomagnetic data. They interpreted the

changes at 193.13 mbsf to be consistent with a long hiatus (Figure 3a). However, Poirier and

Hillaire-Marcel (2011) proposed a new hypothesis for the gap in the record that was based on

osmium isotope stratigraphy, as well as on some of the age-depth markers from Backman et al.

(2008). Rather than being a hiatus, the section was reinterpreted as being a condensed section – a

continuous record of a time of very little deposition (Figure 4b; Poirier and Hillaire-Marcel, 2011). Both age depth models and other paleoenvironmental factors are plotted in a summary figure (Figure 6) to provide a clearer picture of the Arctic Ocean's conditions during the time interval represented by the sediments being investigated by this study.
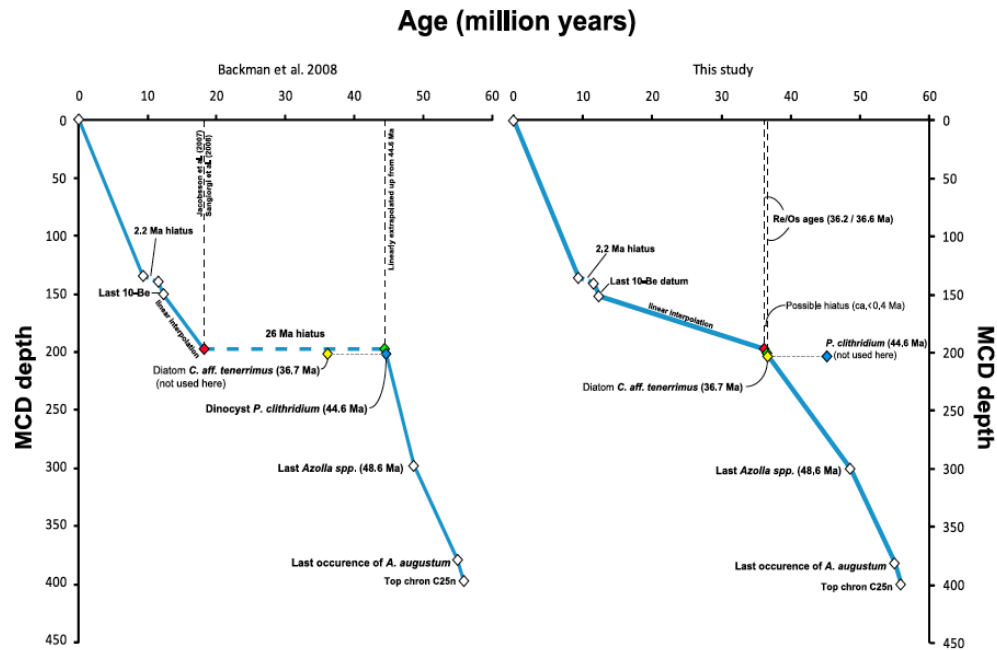
Figure 4: Proposed age/depth models for the Arctic Ocean. (a; left) The graph at left is the original age/depth model showing the gap in the core as a hiatus. (b; right) The graph at right shows the gaps as a continuous record of minimal deposition (after Poirier and Hillaire-Marcel, 2011).

2.3 Ice-rafting History of the Central Arctic

A major discovery of ACEX was that ice initiation in the Arctic occurred at ~46 Ma. Dropstones were recovered from the middle Eocene sediments of the core (Expedition 302 Scientists, 2006). Because the Lomonosov Ridge is isolated from land and is on an offshore bathymetric high, the only way sediments this coarse could have been transported to it would be via ice (icebergs or sea ice). To identify times of ice coverings (Figure 5) two measurements

were made, both related to the sediment. One was quantifying changes in terrigenous sand by weight percent (St. John 2008), and the other was the noting the presence of pebbles on the core surface (Expedition 302 Scientist, 2006).

The section above the hiatus (unit 1/5) has a high rate of terrigenous sand mass accumulation, however, St. John (2008) noted that the sands were potentially reworked and may not represent original depositional conditions. Therefore, these were tentatively disregarded in the St. John (2008) study and no further work was done on the potential ice rafted debris (IRD) sediments from this interval.
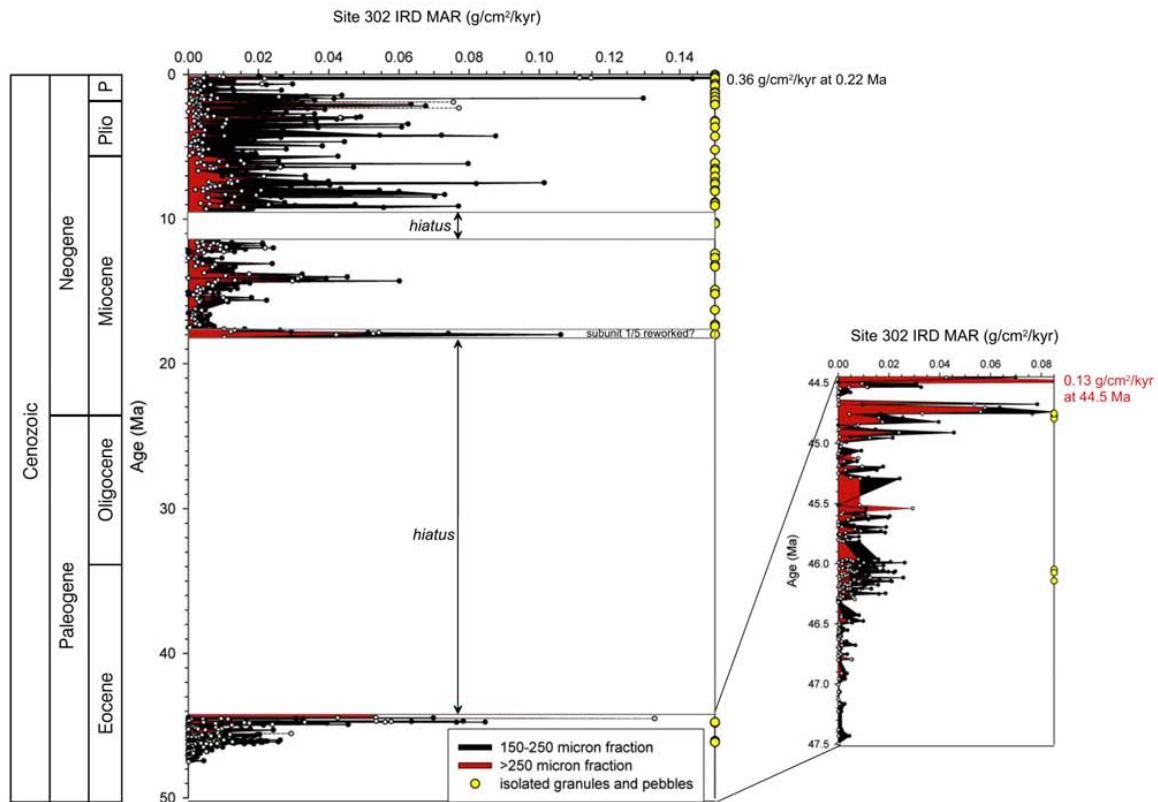

Figure 5: Ice rafted Debris mass accumulation rates plotted versus time. This chart shows ice imitation beginning during the Eocene, over 46 mya. Subunit 1/5 is noted as "reworked?" (St. John, 2008).
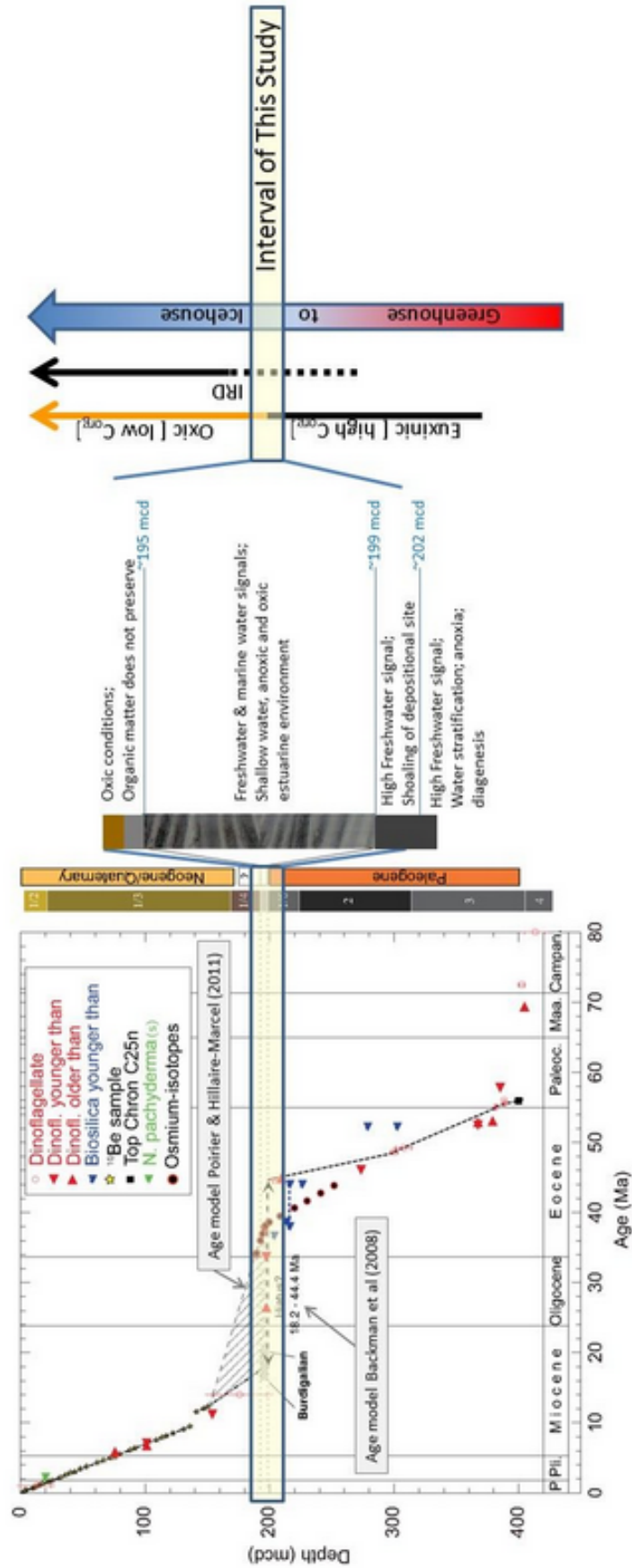
Figure 6: Summary figure of Arctic conditions with the interval of this study highlighted in yellow. Two age models are shown (adapted from O'Regan, 2011): The first interprets the break at 193.13 mbsf to represent a 25 million year hiatus (Backman et al., 2008), while the other interprets it as a condensed section based off of Osmium isotope stratigraphy (Poirier and Hillaire-Marcel, 2011). Stratigraphic units are from Expedition 302 Scientists, 2006. Environmental changes in the Arctic were inferred based on palynological, micropaleontological, and geochemical data (Sangiorgi et al., 2008). The terrigenous coarse sand record indicates that ice rafting initiated prior to the deposition of the "zebra interval", however, data from within in the interval was not considered representative of ice conditions because of the possibility that they had been reworked (St. John, 2008). Organic carbon changes from high to low within the interval of this study indicating a shift from euxinic to oxic conditions (Stein, 2007) (summary figure created by St. John).

3. Data and Methods

3.1 Maximizing the Range of Analysis

With a sample size of only ~10 cc, strategic use of the samples was imperative. In order to complete a broad suite of analyses, each sample needed to be sub-divided and used in a particular order. The flow chart in Figure 7 represents the sub-division and order in which the samples were processed. The methods of analysis were ordered and arranged such that one method would not affect the results of another method. For example, x-ray fluorescence spectroscopy needed to be completed before x-ray diffraction analysis because of the addition of a silicon standard and grain size analysis, and clay x-ray diffraction needed to be completed before the addition of Calgon to the sample.
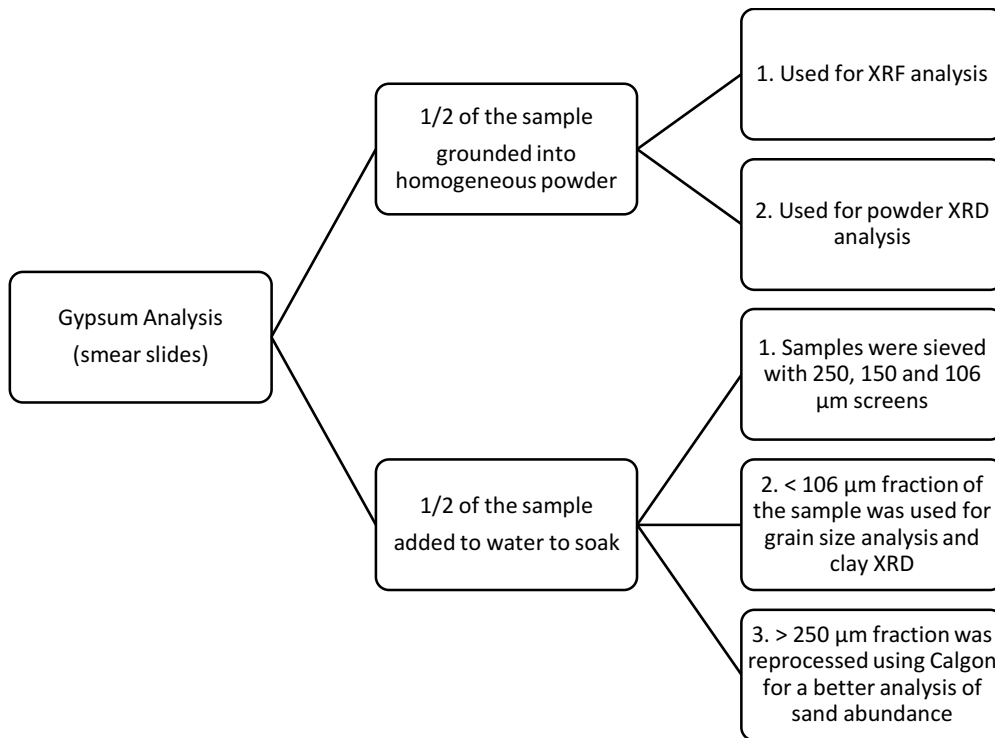

Figure 7: Decision tree for methodology used in this study.

3.2 Smear Slides

A single smear slide was made from subunit 1/4, a black layer from subunit 1/5, a gray layer from subunit 1/5, and subunit 1/6. A small amount of sample was added to a glass slide and mixed with water. This slide was left to dry and a glass cover was adhered to the slide with an epoxy. These slides were then viewed under a petrographic microscope. Because the samples were semi-lithified the creation of the smear slides was difficult. The samples contained clumps and it was difficult to clearly see the mineralogy, however, gypsum was not noted as present.

3.3 X-ray Fluorescence Spectroscopy

X-Ray fluorescence (XRF) is a non-destructive analytical method for measuring the elemental composition of the core samples. The fluorescence emitted by the sample serves to identify the elements present. XRF data gives the relative element abundance in the samples, which can be used to identify stratigraphic changes in composition.

Half of each original bulk sample was gently ground with a mortar to form a homogeneous powder. A Bruker X-Ray Fluorescence Spectroscopy tool and a core track were used for the analyses. Samples were analyzed at both 40 kv and 15 kv voltages (to enhance the detection of different elements) using no filter for a 30 second run. Identification of the elements present was completed using the Artax software. This study focused on major elements that were previously identified during routine, low-resolution shipboard geochemical work (Expedition 302 Scientists, 2006). The most abundant minerals were plotted relative to aluminum in order to normalize the results and compare relative abundances. These ratios were chosen based on previous work done involving this study's subunits (Sangiorgi et al., 2008; Spofforth et al., 2008).

3.4 Powder X-ray Diffraction

Powder x-ray diffraction (XRD) is another analytical method that was used to examine the mineral composition, including the gypsum content in samples. Powder diffraction allows for analysis of bulk samples, and produces diffraction patterns for a bulk composition.

Ten of the powdered samples from the previous XRF analysis were prepared for bulk x-ray diffraction by the addition of a silicon standard. A single sample from both above and below the "zebra interval" were tested for sub-unit comparison and the remaining eight samples were chosen from the "zebra interval" (4 black stripe samples and 4 gray striped samples). 10% sample weight of a silicon standard was added to the samples. The samples were transferred to a 16mm backmount slide and analyzed using the X'Pert Pro XRD software. Peak minerals were searched based on their interplanar d-spacing based on previous work with these subunits (Expedition 302 Scientists, 2006; Vogt, 2009). The area of the element peaks was used to determine relative abundances.

3.5 Sand Composition and Abundance

The remaining half of the samples were used for coarse grain composition analysis and grain size analysis. The original bulk samples were highly indurated. For that reason, they were not further oven dried before obtaining a dry weight. Not drying the samples in an oven, however, introduces some uncertainty, specifically, the possibility that small quantities of pore water might be unaccounted for in the overall sample weight. To address this, unused extra bulk material from 2 samples within subunit 1/5 were used to develop a correction factor. These two samples were oven dried, weighed, and their water content was assumed to represent the water content for other samples from the same lithologic subunit. An average water content was

determined. Applying this water content to the other samples, we were able to calculate an adjusted dried bulk weight for each of the samples.

Sieving steps followed the methods in St. John (2008); the bulk samples were prepared with deionized water and mixed using an ultrasonic bath. Samples were left to soak for an extended period (weeks to months) and were periodically stirred. No deflocculant was added because the fine fraction of these samples was to be used for clay XRD, and a deflocculant would have made it later difficult to flocculate the clays for that form of analysis. The samples were then wet sieved using 105, 150, and 250 μm mesh screens. The greater than 105, 150, and 250 μm fractions were weighed following their being dried in an oven. The less than 105 μm fraction was then used in clay mineral XRD analysis and grain size analysis.

The > 250 μm faction was processed for a second time using sodium hexametaphosphate (i.e., generic Calgon) to deflocculate the clays still attached to some of the grains. These samples were re-sieved with a 250 μm mesh screen, dried and weighed. The coarse sands were analyzed using a binocular microscope. The composition of 100 randomly selected grains from each sample was determined by observation using a binocular microscope. The coarse fraction (sand) weight percentages were calculated using the adjusted bulk sample weight and the weight of isolated and dried > 250 μm faction. Samples with more than 5% semi-lithified sediment clumps remaining even after the dual sample processing steps were not used in the analysis of coarse grain weight percent.

3.6 Clay X-ray Diffraction

If sufficient volume was present, the < 105 μm fraction obtained from the previous compositional work was used to perform clay mineral analysis. Using a centrifuge to remove

larger particles from the remaining sample, an oriented clay mount slide was made. The clays were glycolated prior to XRD analysis, a technique that helps with differentiation of the clay minerals. X-ray diffraction analysis of these oriented samples was used to determine the peak positions of d-spacing, which is the crystallographic parameter used to identify and distinguish the clay minerals present in the samples. The Biscaye (1965) method was used to calculate relative abundances of the minerals.

3.7 Grain Size Analysis

Smear slide observations and bulk powder XRD showed no indication of gypsum being present and so post-depositional mineral precipitation would not be a major factor influencing grain size results (i.e., grain size result should reflect the size distribution of the original deposit). A second assumption was that sieving sufficiently broke down semi-lithified clumps of clay. This assumption may not be entirely valid however, because some clay clumps were observed in the > 250 micron sieves. Nevertheless, grain size analysis was carried out on the samples to look for possible patterns or trends. Using a Beckman Coulter LS 13-320 laser diffraction particle size analyzer, the < 105 μm fraction was analyzed. This fraction of the sample had to be analyzed so as to not interfere with the sand weight percentage. Samples were run with a 10% obscuration using a marine mud model. Obscuration refers to the sample concentration used to complete analysis. Three runs were completed. Grain size counts were used to determine clay, silt, and (very fine) sand percentages as well as mean, median, and mode grain size.

4. Results

4.1 X-ray Fluorescence Spectroscopy

The most abundant elements found in the samples included silicon (Si), potassium (K), titanium (Ti), magnesium (Mn), iron (Fe), manganese (Mg), phosphorus (P), nickel (Ni), strontium (Sr), rubidium (Rb), and cobalt (Co). As shown by figure 8, both subunit 1/4 and 1/6 have a higher average abundance of iron (see note in figure caption) than the "zebra interval". Subunit 1/4 has higher abundances of manganese and strontium, while subunit 1/6 has higher abundances of potassium.
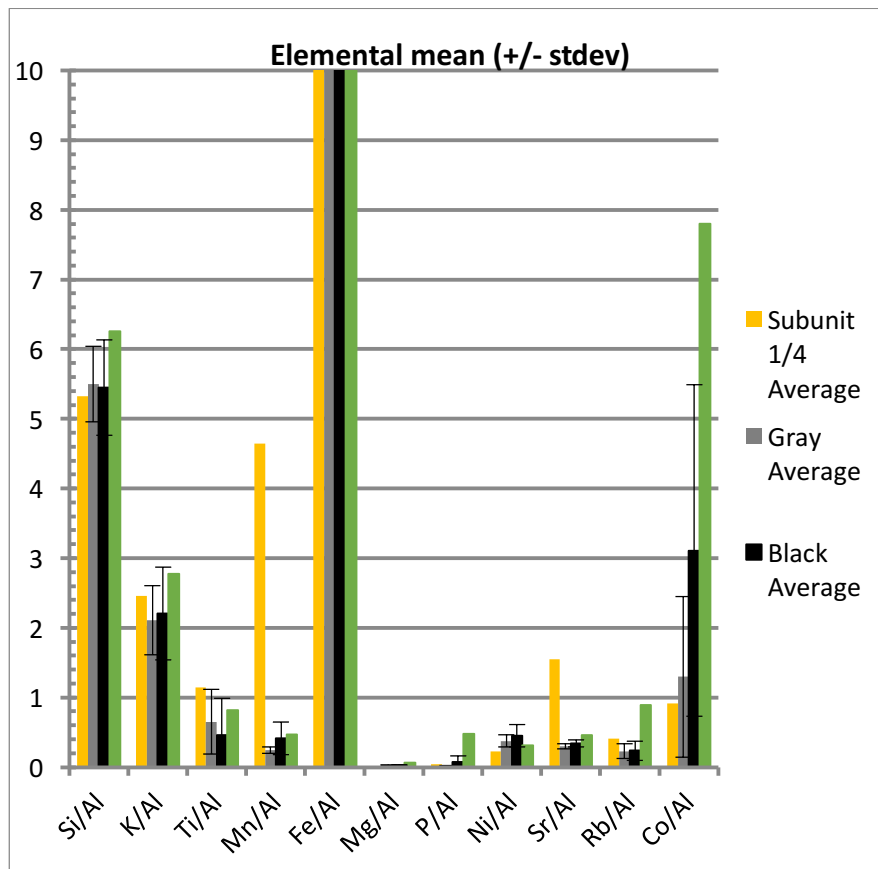

Figure 8: Represents the mean relative abundances of the elements in all three subunits. Subunit 1/5 was divided into both black and gray stripes. The Fe/Al data extends off of the graph and was cut off to increase the clarity of the other elements. The Fe/Al ratios for the layers are listed – Subunit 1/4 average = 59.99, Gray Average = 31.56, Black Average = 47.14, Subunit 1/6 = 149.46

Element abundances for potassium, silicon, and titanium generally match the work done by Sangiorgio et al. (2008) (Figure 9), but the iron data varies. Our data reports subunit 1/4 having high amounts of Fe while the other study shows lower abundance.
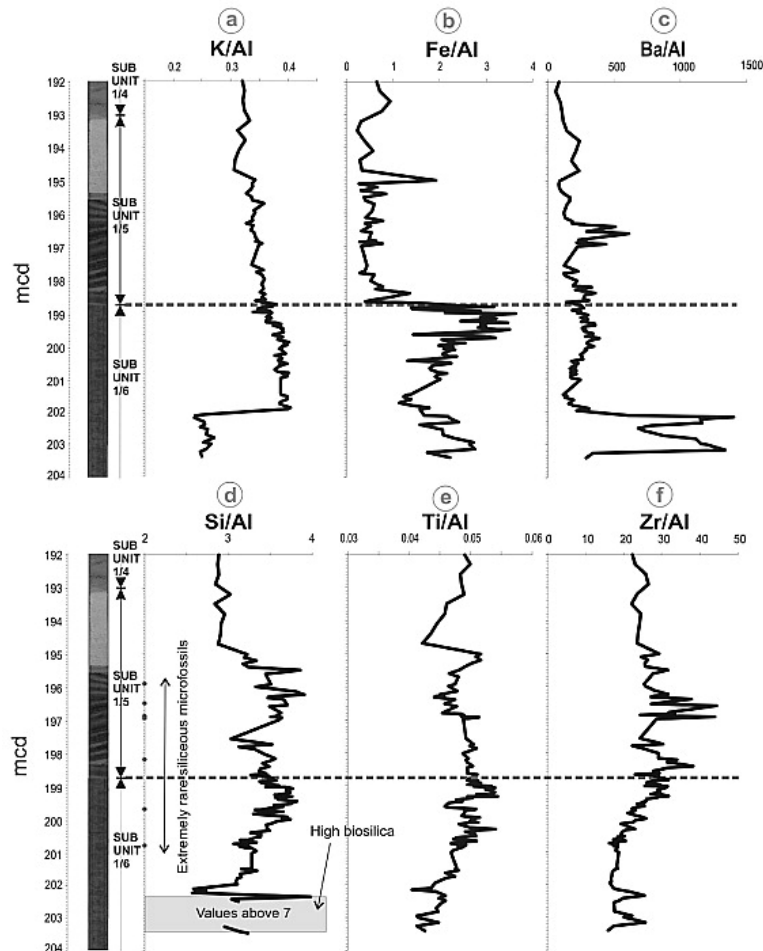
Figure 9: Modified from Sangiorgio et al. (2008). Quantitative X-ray fluorescence measurements were performed on freeze-dried and homogenized sample powders. Elemental ratios plotted against depth. Dashed line indicates the position of the hiatus.

Figure 10 shows the elemental differences between the black and gray stripes from within the "zebra interval". On average, XRF data showed the black layers have more Fe, Co, Ni, K, P, As, Sr, and Mn, whereas gray layers have more Ti.
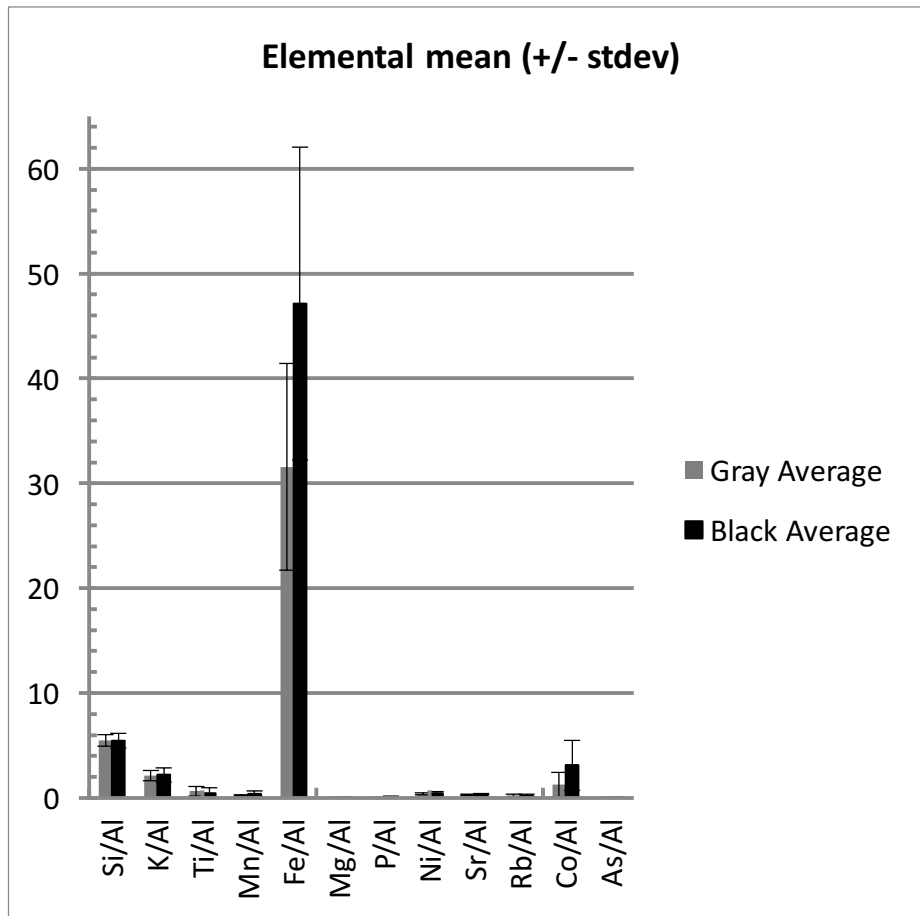
Figure 10: Represents the mean relative abundances of elements in the black and gray stripes from the "zebra interval".

4. 2 Bulk Powder X-ray Diffraction

Due to time constraints (resulting from slow sediment disaggregation), only one sample from above and below the "zebra interval and four black layer and four gray layer samples were analyzed for bulk mineral composition. Over 30 different minerals were identified during the analysis of the bulk samples but many of the minerals varied in their abundances greatly between the samples. Plagioclase, quartz, and muscovite were the most abundant minerals and were present in all of the samples.
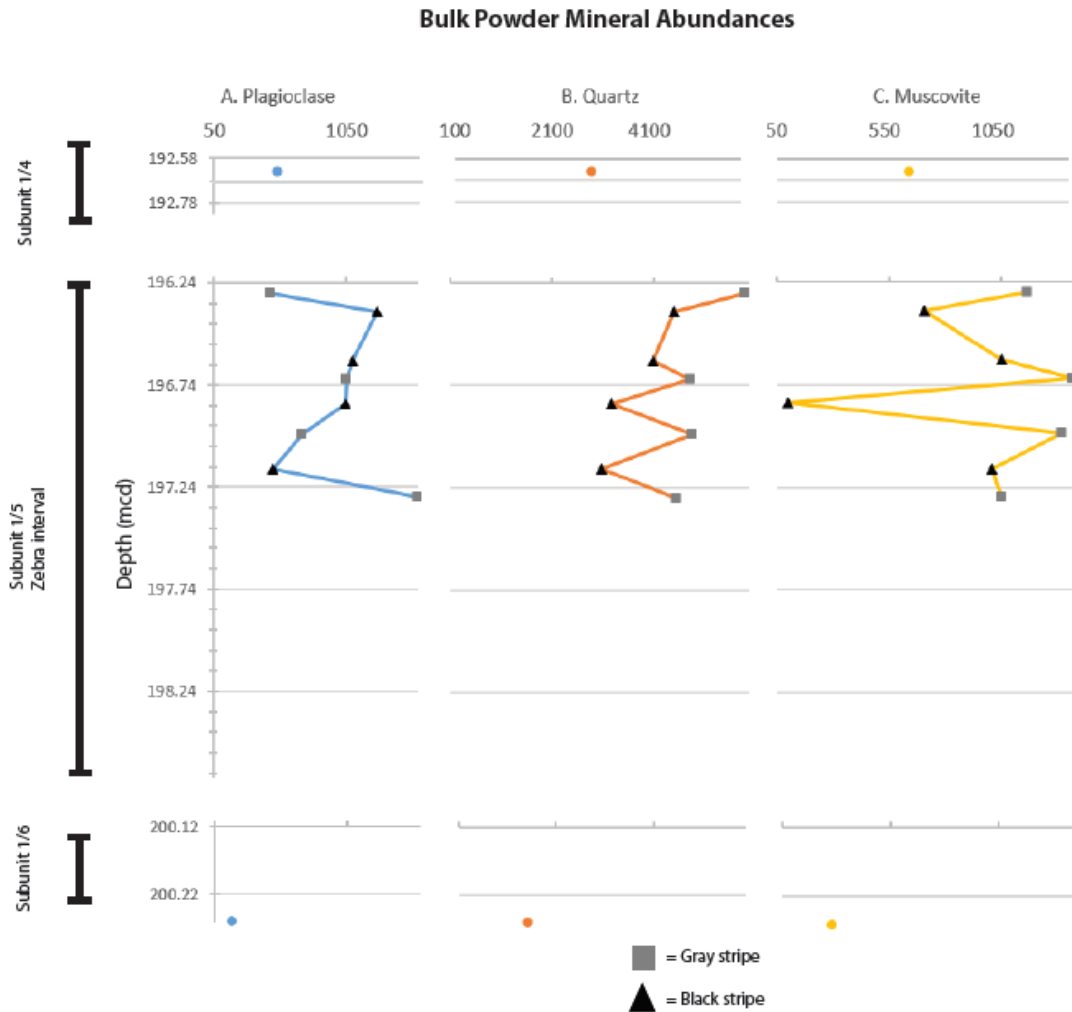
Figure 11: represents variations in abundance (peak area) of plagioclase, quartz, and muscovite from a subset of samples

The data show that the gray layers from the "zebra interval" have higher relative abundances of quartz and muscovite than the black layers. This difference is puzzling because with an increase in quartz, we would expect an increase in grain size associated with the gray layers, however we see no consistent difference in grain size between the gray and black layers (see section on grain size results). The data also indicate that subunit 1/6 has generally lower abundances of all three elements compared to the "zebra interval". More samples will need to be run in order to make more accurate interpretations of these data.

4.3 Sand Composition and Abundance

There was little difference between the three subsections of samples in terms of coarse grain composition. In all samples, except samples with a significant amount of semi-lithified sediment clumps, the coarse grain fraction was dominated by quartz (clearly seen in figure 12). The quartz that was present in the samples showed rounding. The other grains present in the samples were feldspar, lithics, micas, and sedimentary rock fragments. One notable difference was the abundance of iron stained quartz (Figure 12A) in subunit 1/4, which was not prevalent in the other two subunits.

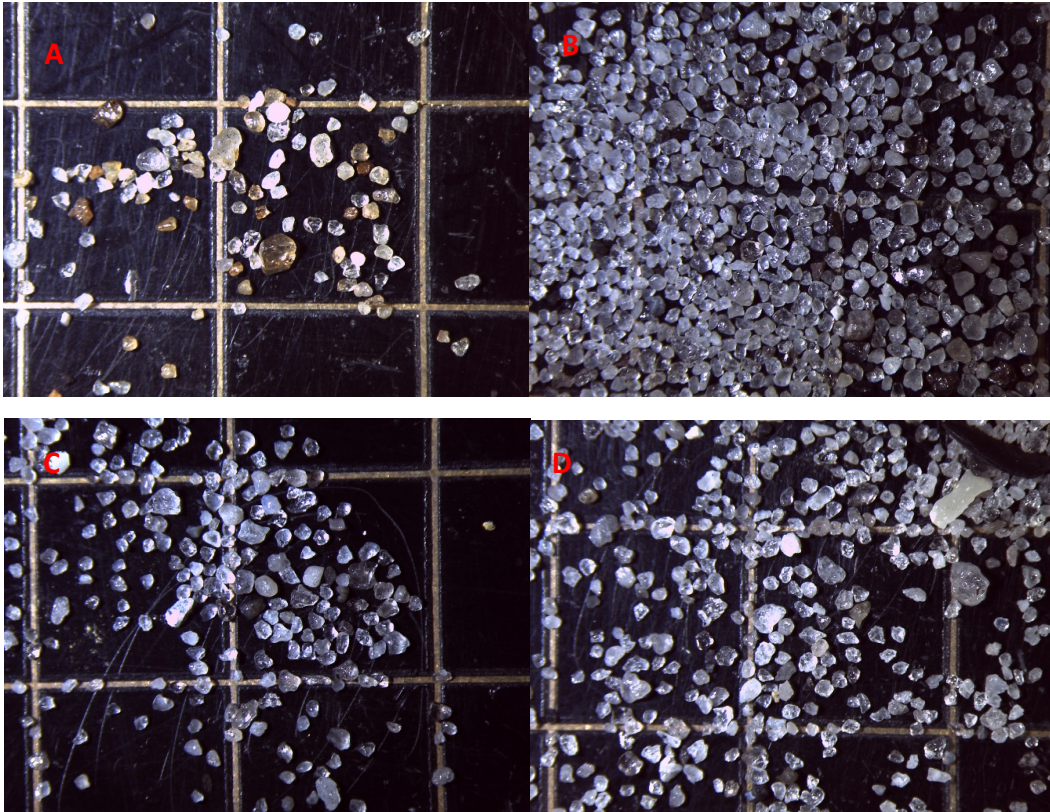*Figure 12: Photographs representative of the coarse grain fraction of each subunit. A – subunit 1/4 - sample 302 2A 44x 71-72cm >250 μm fraction at 25x magnification. B – subunit 1/5 - sample 302 2A 45x 43-44 cm >250 μm fraction at 25x magnification (gray stripe). C – subunit 1/5 - sample 302 2A 45x 130-131 cm >250 μm at 25x magnification (black stripe). D – subunit 1/6 sample 302 2A 46x2 105-106 μm fraction at 25x magnification.*
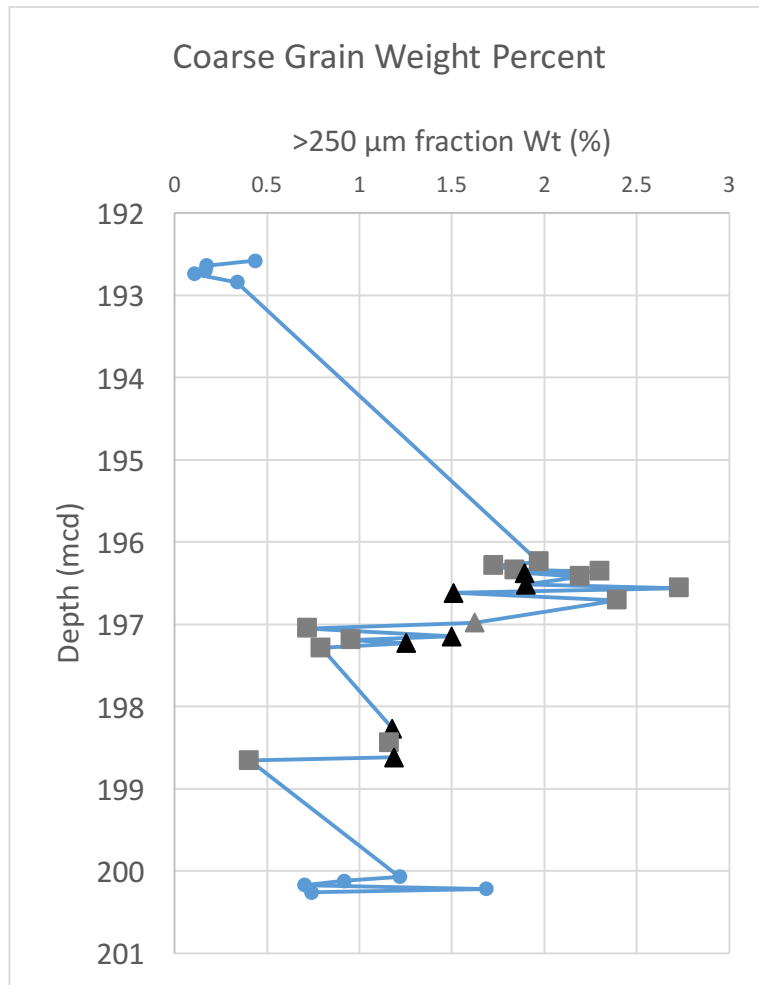
Figure 13: Coarse grain weight percentage plotted against depth. Gray squares represent gray stripes and black triangles represent black stripes. The data points above the "zebra interval" represent subunit 1/4 and the data points below represent subunit 1/6.

The coarse grain weight percentages from subunit 1/6 to the first half of the "zebra interval" remains consistent, generally ranging from 0.5% to 1.5%. About half way through the "zebra interval", the weight percentage increases. This change increased the weight percentages of the coarse-grained sands to between 1.5% and 2.7%. Above the "zebra interval", the coarse grain weight percentages drop dramatically. The weight percentages of samples in subunit 1/4 ranges from 0.1% to 0.43%. There is no clear trend between the black and gray stripes of the "zebra interval". There was no trend in sand abundance within the "zebra interval". The color of

the stripe did not affect the sand weight percent of the sample. This data is consistent with the work done by St. John (2008) (figure 13). Similarly to the data collected for the present study, the 2008 study reported an increase in sand abundance in the upper part of subunit 1/5, and a large decrease in subunit 1/4.
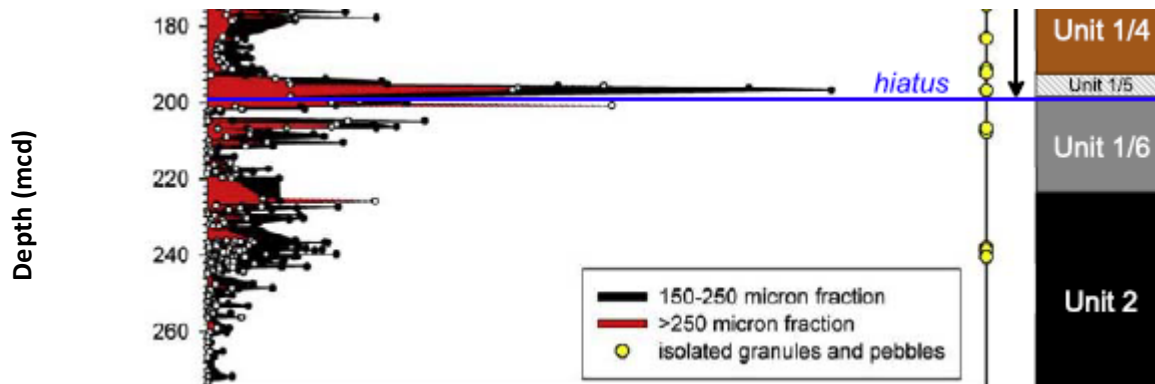
Figure 14: Terrigenous sand weight percentages from site 302 surrounding the major hiatus (St. John, 2008).

4.4 Clay X-ray Diffraction

Clay composition analysis was conducted for samples that yielded a significant amount of grains < 2 μm diameter (13 out of 30 samples). Many of the samples from within the zebra unit and all of the samples from subunit 1/6 did not produce a sustainable amount of clay material and clay slides were not possible to make. While samples from subunit 1/4 did have a higher abundance of clay than subunit 1/5 and 1/6 (Figure 17), the samples that did not produce clay slides contained at least 13% clay grains. There was likely an issue with volume of the sample available which was puzzling considering the lithology of both units was silty-clay.

Subunit 1/5 has varied clay mineralogy; however, the gray vs black layers within subunit 1/5 show no distinct differences in clay mineralogy (Figure 16). This suggests a consistent

dominant provenance during the deposition of the light vs dark zebra layers, which is the

Kara/Laptev Sea region. Based on Vogt's (2009) mineral provenance map (Figure 15), the shift

from smectite-dominated (upper subunit 1/5) to illite-dominated (subunit 1/4) may suggest a shift

in provenance from the Kara/Laptev Sea region to the east Siberian and/or Canadian Arctic

Ocean margins. The abundance of smectite in subunit 1/5 suggests an environment when there

was a dominant Transpolar Drift (TD) transporting the smectite material. The Laptev Sea area is

a source area for Smectite and the Transpolar Drift would be capable of moving the material

from that region north to the Lomonosov Ridge (Vogt, 2009). In order for the illite to be

deposited at site 302 the Beaufort Gyre (BG) would need to transport the illite from the Siberian

and/or Canadian shield. Quartz is present in both provenance regions making the areas

appropriate sources for the sand fraction of the samples.
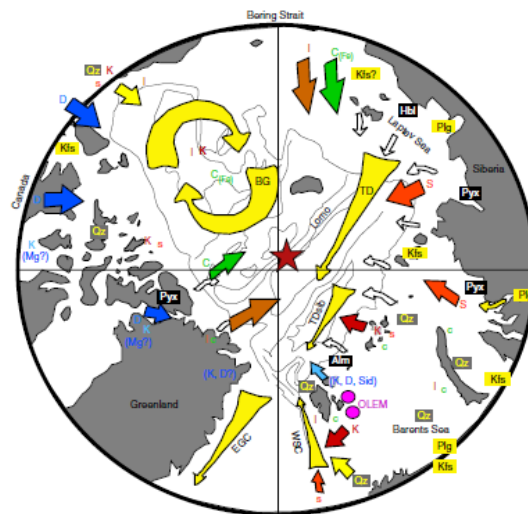
Figure 15: Provenance of minerals and mineral groups in the Arctic (Vogt, 2009). Site location is marked by red star. White arrows = downslope sediment transport mainly through troughs. Alm = almandine, C(Fe) = Fe-rich chlorite, D = dolomite, Hbl = hornblende/amphibole, I = illite/ mica, blue K = calcite, red K = kaolinite, Kfs = K-feldspar, Mg = Mg-rich calcite, OLEM = mixed-layer clay, Plg = plagioclase, Pyx = pyroxene, Qz = quartz, S = smectite, Sid = siderite. BG = Beaufort Gyre, EGC = East Greenland Current, Lomo = Lomonosov Ridge, TD = Transpolar Drift, TDsib = Siberian branch, WSC = Westspitzbergen Current
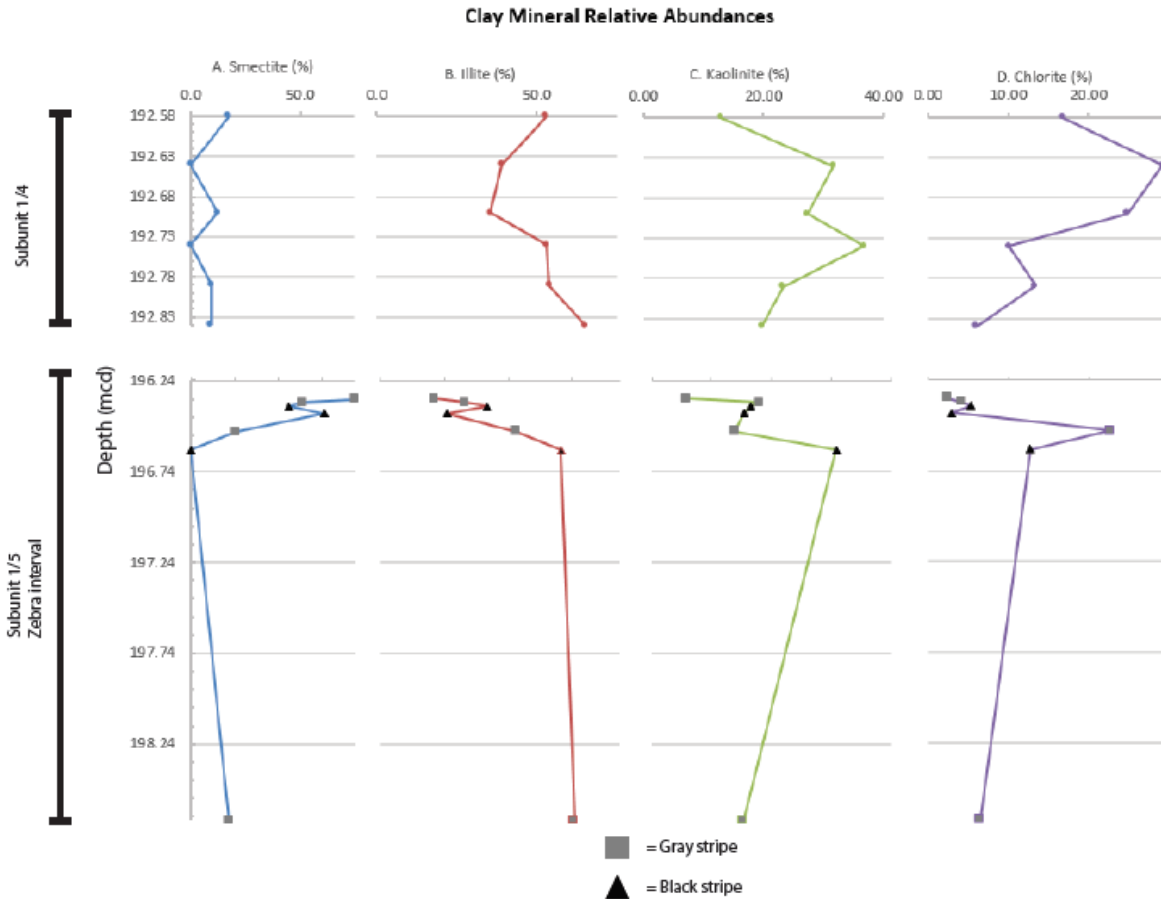
Figure 16 – Clay abundances plotted against depth for subunit 1/4 and 1/5. Subunit 1/6 did not produce enough volume to conduct clay XRD analysis.

Additionally, there is a clear shift of increasing amounts of smectite in the "zebra interval" and then it decreased significantly when subunit 1/4 begins. This same increase followed by a drop occurs in the sand abundance data too. This pattern may indicate a stronger input of material from the Kara/Laptev Sea region from the Beaufort Gyre.

4.5 Grain Size Analysis

Grain size analysis was completed for the < 105 μm fraction. The analysis was not done on samples that had been treated with Calgon because the same sub-fraction was used to

complete clay XRD. This limits our ability to make definitive interpretations because the data likely does not show true grain size. All 35 samples were run and from the data percent clay, cohesive silt, sortable silt and sand, average, median, and mode grain size, and standard deviation of the data and was obtained.

There is no discernible difference in grain size between the black and gray stripes. The layer appearance within the zebra interval would suggest a change in current to account for the cross bedding, however there is no grain size data to suggest this change between the layers. Figure 16 B & C represent average black and gray stripe grain distribution. These two graphs illustrate the similarity in grain size diameter seen between the two different colored stripes. Subunit 1/6 (D) is more similar in grain distribution to the "zebra interval" than is overlying subunit 1/4.

Using standard deviation as a way to interpret sorting, the "zebra interval" is more poorly sorted in comparison to the other subunits, meaning that there is a wide range of grains sizes within the samples. This difference between the subunits in regards to sorting may point to a change in energy. This change in energy may be associated with wave erosion or tidal forces coming from shallow water that could have produced the hiatus (Sangiorgi et al., 2008). While an increase in energy would align with strong bottom currents (Moore et al., 2006) capable of reworking the "zebra interval", the presence of clays in the samples argues against that explanation, because the currents would have winnowed them away.
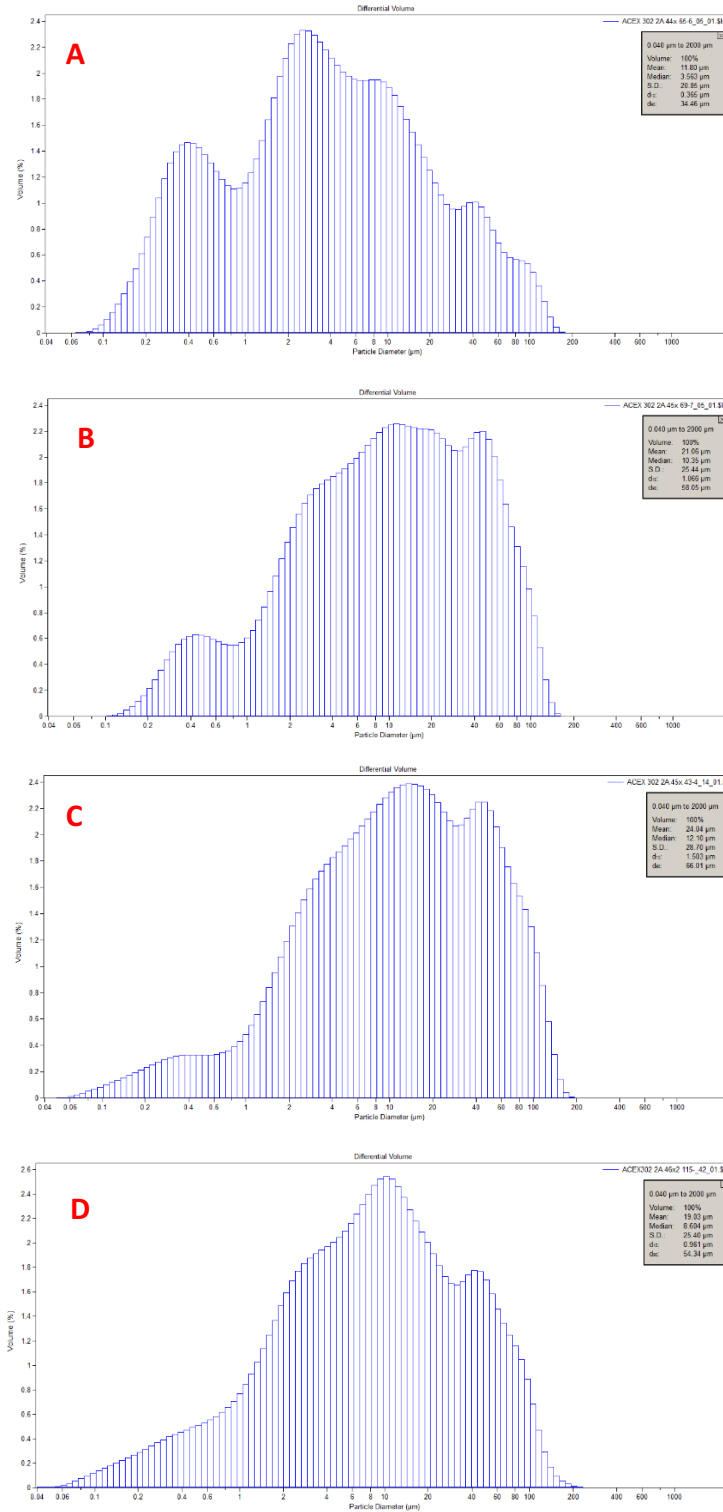
Figure 17 – These four graphs show a representative distribution of grain size (particle diameter v. volume) from each unit. Grain size distribution is shown in the following order - subunit 1/4, subunit 1/5 black stipe, subunit 1/5 gray stripe, subunit 1/6
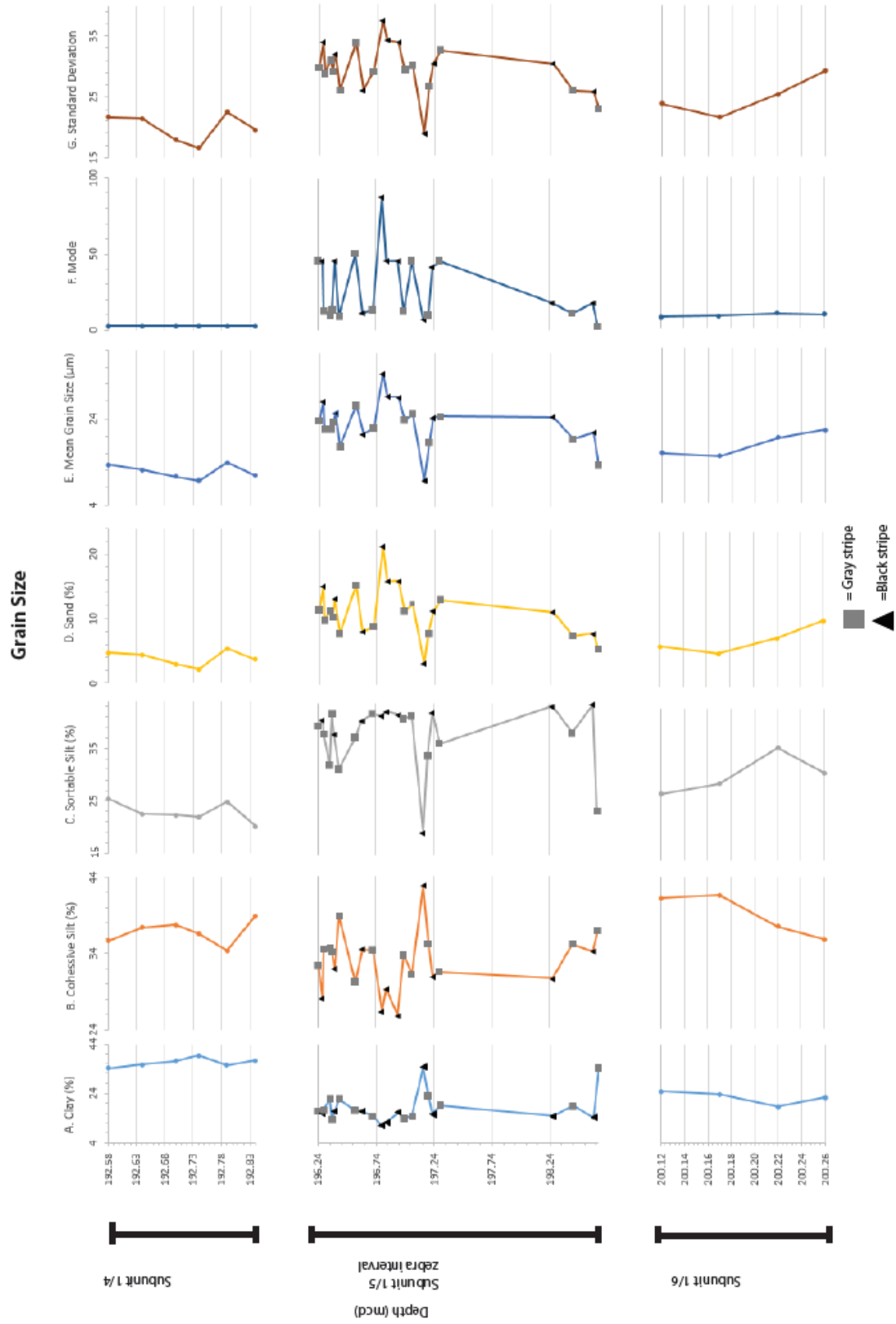
Figure 18 – Grain size data from the three subunits of interest.

5. Conclusions

5.1 Limitations of the Study

The sediment samples from the "zebra interval" were highly indurated and therefore difficult to sieve, even after soaking for weeks in DI water. We did not want to treat the full bulk samples with a deflocculant (e.g., Calgon) because that would make it difficult subsequently to make oriented mounts for clay mineral XRD analyses. Even without Calgon, however, the creation of oriented clay slides was nonetheless not without difficulty because of a lack of volume of clay-sized grains in many of the samples. Additionally, because the samples were so difficult to sieve, the grain size analysis may not be an accurate representation of sample grain sizes. The decision was eventually made to treat and then re-sieve the samples following clay and grain size analysis. Even with the additional treatment with Calgon, some samples still did not completely disaggregate, and some semi-lithified clumps were present in the coarse grain fraction. These semi-lithified clumps had to be taken into consideration when analyzing the sand abundance. Samples with more than 5% abundance of semi-lithified clumps were not used in the analysis of sand abundance.

Additionally, when preparing the samples for clay XRD, many of the samples within, and all of the samples below, the "zebra interval" did not have enough clay-sized (<2 μm diameter) material for analysis making any conclusions made incomplete. Grain size results using the Laser Diffraction Particle Size Analyzer may also have been impacted because the <106 μm fraction may not have been fully disaggregated and therefore did not fully reflect the true grain distribution of the sample.

5.2 Interpretations

Although there are some differences within and between the elemental data and the mineralogy of the black and gray stripes within the "zebra interval", they are minimal. Additionally, there is no consistent pattern with in the grain size data. We cannot confidently infer any differences in provenance within the "zebra interval" (subunit 1/5). This implies that the sediments were deposited in a consistent environment. The roundedness observed, potentially caused by back and forth reworking, on the dominate quartz sand grains supports deposition in a shallow water environment, as suggested by Sangiorgio et al. (2008). The color changes within subunit 1/5 may have occurred post-depositionally, reflecting changes in organic carbon content and alternating oxic-anoxic (Eh) conditions in an estuary setting. One process that might cause repeated cycles of oxic-anoxic conditions in an estuary would be a pattern of density stratification (producing anoxia in the bottom waters) and seasonal overturn (renewing the oxygen). Seasonal sea ice formation might play a role in this.

A shift in provenance can be inferred between subunit 1/5 and 1/4. There is an increase in sand and smectite abundance towards the top of the "zebra interval" and a decrease at the beginning of subunit 1/4. This pattern not only indicates a change in source material from the Kara/Laptev sea to the Siberian and/or Canadian margin, but it also indicates a change in current transport. The smectite and the higher abundance of sand grains were likely transported from the Kara/Laptev sea regions by the Transpolar drift, whereas the deposition of illite and a decrease in sand abundance would represent the Beaufort Gyre becoming an additional important mode of sediment delivery from the Siberian and/or Canadian margin.

Additionally, the increase in sand abundance in the upper part of subunit 1/5 and the large decrease in subunit 1/4 are consistent with the results from St. John (2008). As noted in

that study, the sand grains within unit 1/5 were likely reworked and thus are not reliable IRD indicators. The results obtained from this study point to a shallow water setting for the depositional environment of these samples, and therefore reinforce the conclusion that the sands in this unit would not have utility as an indicator for possible IRD.

5.3 Outstanding Questions

There are several inconsistencies within the data that have left outstanding questions regarding the deposition of the "zebra interval".

If the black and gray layers are post-depositional, could overturning of the water column cause the alternating bands?

Overturning of the water column could account for the color changes within the "zebra interval". When the water column is stratified the sediments would be deposited in anoxic conditions, while a mixed water column would allow the sediments to be deposited in oxic conditions. The changing of these two conditions could be a cause of the alternating bands. The overturning of a water table can be a seasonal occurrence but it also can be caused by ice. The appearance of ice would block winds from mixing the water and therefore cause anoxic conditions. Alternatively, when sea ice forms salts are largely excluded, causing the underlying surface waters to increase in salinity and therefore become denser and sink. This would cause water column overturn and renew the deeper waters with oxygen. The 26-million-year hiatus that the "zebra interval" sits on top of covers a transition from a greenhouse to icehouse earth and sea ice diatoms and IRD analysis from lithological unit 2 (the unit below this study's area) indicate the onset of seasonal offshore ice at the Lomonosov ridge (Stickley et al., 2009). Seasonal ice

would be a reasonable mechanism for overturning the water column, however this mechanism would not explain the truncation of the layers.

If the black and gray layers are not post-depositional, why is there no change in grain size?

If the black and gray layers are not post-depositional and actually a change in seasonal fluctuation, we would expect to see a change in grain size. If these layers were tidal couplets, we would be able to see a distinct change in energy between the two colors. For example, during the spring flood the energy would be increased and we would expect to see an increase in grain size. During Ebb we would see a decrease in energy and a decrease in grain size. The color banding of these samples do not reflect the increase/decrease grain size pattern that would be associated with tidal couplets. It is possible however that the issues faced with processing have not allowed for grain size of the samples to be truly represented. In order to confirm if these colored layers are or are not post depositional, another method must be used to examine grain size.

5.4 Further Research Opportunities

A completion of bulk powder X-ray diffraction would lend itself to a clearer idea of the mineralogy of the samples. With the 10 samples now completed, it is difficult to conclusively determine patterns in the data so further XRD work could eliminate uncertainty. The addition of this data would further support the possibility of a change in provenance interpreted from the clay XRD data.

Further work including the examination of quartz grain surface textures may provide insight to the depositional history of these samples. Examining grain surface textures within the interval can be used in comparison to the St. John study (2008) in which grains from above and

below the "zebra interval" have been attributed to sea ice or iceberg transport. Differences in quartz grain textures (e.g., significant increase in ground rounding, and dissolution) within the "zebra interval" may support a complex transport history, with significant reworking that would be expected in an estuarine environment.

Additionally, due to the lithified nature of the samples, a new method could be used to address the grain size aspect of these samples. It is possible that creating thin sections of the samples across the core could be used to determine grading. Grading throughout the "zebra interval" could provide an insight into the environment in which the samples were deposited.

This shallow depositional setting was a challenging setting for continuous recovery. Changes in relative sea level - whether from sea level fall as glaciers were expanding on land in the Arctic region (St. John, 2008) and in Antarctica (Carter et al., 2017), or from changes in the Lomonosov ridge subsidence (Moore et al., 2006; Sangiorgi et al., 2008; Kaminski 2009) – resulted in a highly discontinuous/limited record. This puzzling time of paleoceanographic and paleoclimatic transition will be investigated further in upcoming IODP Expedition 377, which aims to recover a complete record of Eocene-Miocene time at a nearby location more conducive to continuous deposition and preservation.

Appendix A

Core	Section	Top Depth (cm)	Bottom Depth (cm)	Volume	MBSF Top	Remarks
IODP 302 (ACEX) Sample Information						
44	1	59	60	10	192.58	
44	1	65	66	10	192.64	
44	1	71	72	10	192.7	
44	1	75	76	10	192.74	
44	1	80	81	10	192.79	
44	1	85	86	10	192.84	
45	1	31	32	10	196.24	gray
45	1	34.5	36	10	196.275	black
45	1	36	37	10	196.29	gray
45	1	41	42	10	196.34	gray
45	1	43	44	10	196.36	gray
45	1	45	46.5	10	196.38	black
45	1	49	50	10	196.42	gray
45	1	59	60	10	196.52	black
45	1	63	65	10	196.56	gray
45	1	69	70	10	196.62	black
45	1	78	79	10	196.71	gray
45	1	86	88	10	196.79	black
45	1	90	91	10	196.83	black
45	1	100	101	10	196.93	black
45	1	105	106	10	196.98	gray
45	1	112	113	10	197.05	gray
45	1	122	124	10	197.15	black
45	1	126	127	10	197.19	gray
45	1	130	131	10	197.23	Black
45	2	5	7	10	197.29	gray
46	1	70	71	10	197.7	Black
46	1	87	88	10	197.87	Gray
46	1	105	107	10	198.05	black
46	1	109	110	10	198.09	Gray
46	2	100	101	10	199.5	
46	2	105	106	10	199.55	
46	2	110	111	10	199.6	
46	2	115	116	10	199.65	
46	2	119	120	10	199.69	

Bibliography

Backman, J., Jakobsson, M., Frank, M., Sangiorgi, F., Brinkhuis, H., Stickley, C., O'Regan, M., Løvlie, R., Pälike, H., Spo_orth, D., Gattacecca, J., Moran, K., King, J., Heil, C., 2008. Age model and core-seismic integration for the Cenozoic ACEX sediments from the Lomonosov Ridge. Paleoceanography 23, doi:10.1029/2007PA001476

Carter, A., Riley, T., Hillenbrand, C., Rittner, M., 2017. Widespread Antarctic glaciation during the Late Eocene. Earth and Planetary Science Letters, v. 458, p. 49-57. https://doi.org/10.1016/j.epsl.2016.10.045

Expedition 302 Scientists, 2006, Expedition 302 summary: Proceedings of the Integrated Ocean Drilling Program, v. 302, p. 22 pp., doi:10.2204/iodp.proc.302.101.2006.

Kaminski, M., Silye, L., and Kender, S., 2009, Miocene deep-water agglutinated Foraminifera from the Lomonosov Ridge and the opening of the Fram Strait: Micropaleontology, v. 55, p. 117-135.

Moore, T.C., and the Expedition 302 Scientists, 2006. Sedimentation and subsidence history of the Lomonosov Ridge. In Backman, J., Moran, K., McInroy, D.B., Mayer, L.A., and the Expedition 302 Scientists, Proc.IODP, 302: Edinburgh (Integrated Ocean Drilling Program Management International, Inc.). doi:10.2204/iodp.proc.302.105.2006

O'Regan, M., et al. (2008), Mid-Cenozoic tectonic and paleoenvironmental setting of the central Arctic Ocean, Paleoceanography, 23, PA1S20, doi:10.1029/2007PA001559

O'Regan, M., 2011. Late Cenozoic Paleoceanography of the Central Arctic Ocean. IOP Conf. Series: Earth and Environmental Science 14, doi:10.1088/1755-1315/14/1/012002.

Poirier, A. and Hillaire-Marcel, C., 2009. Os-isotope insights into major environmental changes
of the Arctic Ocean during the Cenozoic. Geophys. Res. Lett. 36, L 11602, doi:
10.1029/2009GC037422

Sangiorgi, F., Brumsack, H.J., Willard, D.A., Schouten, S., Stickley, C.E., O'Regan, M.,
Reichart, G.J., Sinninghe Damsté, J.S., and Brinkhuis, H., 2008, A 26 million year gap in
the central Arctic record at the greenhouse-icehouse transition: Looking for clues:
Paleoceanography, v. 23, p. 1–13, doi: 10.1029/2007PA001477.

St. John, K., 2008. Cenozoic ice-rafting history of the Central Arctic Ocean: Terrigenous sands
on the Lomonosov Ridge. Paleoceanography, doi:10.1029/2007PA001483.

Stein, R., 2007. Upper Cretaceous/Lower Tertiary black shales near the North Pole: Organic-
carbon origin and source-rock potential. Marine and Petroleum Geology 24, 67-73

Stickley, C. E., St John, K., Koc, N., Jordan, R. W., Passchier, S., Pearce, R. B., & Kearns, L. E.
(2009). Evidence for middle eocene arctic sea ice from diatoms and ice-rafted debris.
Nature (London), 460(7253), 376-379. doi: http://dx.doi.org?10.1038/nature08163

Spofforth, D.J.A., Pälike, H., and Green, D., 2008. Paleogene record of elemental concentrations
in sediments from the Arctic Ocean obtained by XRF analyses. Paleoceanography,
23(1):PA1S09. doi:10.1029/2007PA001489

Vogt, C., 2009. Data report: semiquantitative determination of detrital input to ACEX sites based
on bulk sample X-ray di_raction data. InBackman, J., Moran, K., McInroy, D.B., Mayer,
L.A., and the Expedition 302 Scientists, Proc. IODP, 302: Edinburgh (Integrated Ocean
Drilling Program Management International, Inc.). doi:10.2204/iodp.proc.302.203.2009